Heart Vessels (1998) 13: 95–101

Heart and Vessels

Thickness, taper, and ellipticity in the aortoiliac bifurcation of patients aged 1 day to 76 years

Neil F. MacLean[1] and Margot R. Roach[1,2]

Departments of [1]Medical Biophysics and [2]Medicine, The University of Western Ontario, London, Ontario, Canada N6A 5C1

Summary. Lumen area, ellipticity, and wall thickness were measured in the aortoiliac bifurcations obtained at autopsy from 14 patients aged between 1 day and 76 years. The method involved freezing pressure-fixed, stained bifurcations on the stage of a refrigerated microtome and then looking at the block face while sections were removed. Area change was normalized over segment length to produce a value of either taper (narrowing, in mm^2/mm), or flare (expansion). The aortoiliac bifurcations were divided into three regions based on the area changes: an apical region corresponding to the bifurcation apex (taper = 2.96 ± 0.80 mm^2/mm), a preapical region (flare = 3.58 ± 0.87 mm^2/mm), and the postapical region (flare = 0.82 ± 0.80 mm^2/mm). Preapical lumen ellipticity showed that the anterioposterior diameter was always less than the lateral diameter, while the degree of ellipticity increased with age. Average circumferential wall thickness, assessed in polar coordinates, decreased between 0° (right lateral) and 120°, while a significant increase in wall thickness was present between 120° and 200°. The most striking difference was found in the 1-day-old, which was very thin posteriorly. This detailed geometric analysis of the aortoiliac bifurcation suggests that taper, flare, and variations in both circumferential and longitudinal wall thickness need to be considered when trying to correlate physical factors in the aorta with the precise location of atherosclerotic lesions and wall remodeling.

Address correspondence to: N.F. MacLean

Financial support was provided by the Heart and Stroke Foundation of Ontario, the Terence W. Gilmore Memorial Scholarship, the Medical Research Council of Canada, and the Cadillac Fairview Corporation

Received July 1, 1998; revision received September 3, 1998; accepted September 11, 1998

Key words: Wall thickness – Taper – Ellipticity – Aortoiliac bifurcation

Introduction

The size, and presumably the shape, of the aorta and other large arteries obviously must change with growth, although details are not available. Studies by Zarins et al. [1] showed in a monkey A-V fistula model that despite increasing blood flow velocity in the right iliac artery, a constant level of wall shear stress was maintained via a compensatory mechanism which increased lumen diameter. Brownlee and Langille [2] showed that left-to-right carotid anastomosis in rabbits of various ages produced lumen size changes with flow, and that this was more dramatic in 5- to 6-week-old rabbits than in adult rabbits. The coupling of artery remodeling that exists between lumen diameter and wall thickness in disease states is confounded by changes that occur due to aging.

No detailed studies of lumen geometry associated with wall thickness around the circumference have been made to our knowledge, and this study was designed to determine how the infrarenal aorta changed from birth to old age in a series of 14 patients. The infrarenal aorta is a major site of both atherosclerosis and aneurysm formation, and both are associated with local changes in lumen and wall dimensions. This region also undergoes huge changes is flow immediately after birth when the low resistance placental circulation is removed.

The method used is a modification of one developed previously in our laboratory to assess changes in lumen area of porcine renal arteries and human cerebral arteries [3]. It allows measurements of both lumen area and wall thickness, and so has an advantage over clinical imaging methods which give good values of lumen size,

but do not show the wall thickness accurately. Standard histological techniques are useful for measuring wall thickness but not lumen size due to sectioning artifacts.

The key parameters to be assessed are lumen area, ellipticity, and wall thickness as a function of both distance from the renal arteries to the aortic bifurcation, and also wall thickness measured around the circumference of the vessel.

Materials and methods

The human aortoiliac bifurcation was chosen for this study because it is a large-caliber, elastic Y-bifurcation that is predisposed to arterial diseases such as atherosclerosis and aneurysms. It undergoes large geometrical changes following birth and was available at autopsy. Autopsy samples were collected at the Children's Hospital of Western Ontario and the London Health Sciences Centre from 14 patients ranging in age from 1 day (0.003 years) to 76 years (Table 1). The cause of death of these patients was not related directly to abdominal aortic disease. Only the 61-year-old had evidence of hypertension with a thickened left ventricular wall.

Human aortas were collected and loose adipose tissue was dissected off. The arteries were made pressure-tight by tying-off both common iliac arteries and all of the side branches. Each sample was pressure-fixed for 3 h with 10% buffered formalin under static pressure conditions by connecting the infrarenal aorta to a pressure reservoir.

Calcification associated with atherosclerotic disease was present in five of the adult samples that were studied (i.e., the 44-, 59-, 61-, 73- and 76-year-old patients). Deposits were solubilized by suspending each vessel in 12% ethylenediaminetetraacetic acid (EDTA, pH = 7.0) for 1 week. This method gives superior results compared with use of conventional acid decalcifying agents since it avoids tissue hydrolysis [4].

The crux of the method is to freeze the bifurcations on the stage of a freezing microtome, and then look at the block face as sections are removed. This avoids the usual histological artifacts of compression and folding. To enhance edge-detection and the accuracy of lumen and wall thickness measurements, the bifurcations were stained with 0.01% acid fuchsin (20 h).

The decalcified, stained vessels were mounted with the common iliac arteries toward the top and with the parent branch perpendicular to the stage of a refrigerated sledge microtome (Leitz Kryomat, $T = -30°C$). Two thin-walled styrofoam cylinders provided both insulation and a rigid form in which the artery was embedded. The embedding compound was poured into the lumen of the vessel and then around the base of the sample while liquid nitrogen was poured over the top surface. This produced rapid freezing from the top of the block, downwards, while the refrigerated microtome froze the block from the bottom, upwards. The black was allowed to freeze for 1 h to reach thermal equilibrium prior to sectioning. Sections were removed from the block face at 10-μm increments in juvenile samples and at 40-μm increments in adult samples. A vertically mounted video camera (Hitachi KP M1U, Tokyo, Japan) recorded the block face while an S-VHS video recorder (Panasonic AG 7350, Osaka, Japan) stored the images for future analysis. The video-taped images were digitized (Data Translation, DT2853, Marlboro, MA, USA) with an IBM-compatible computer and were analyzed using custom software. Prior to sectioning, the imaging system was calibrated with a grid consisting of 4 × 4-mm squares that were recorded at blade height, and then digitized. The number of pixels per mm was measured in both the vertical and horizontal directions and allowed the conversion from units of $(\text{pixels})^2$ to $(\text{mm})^2$.

Table 1. Patient data

Age of patient (years)	Sex	Cause of death	Left ventricular wall thickness (mm)
0.003	F	Stillborn	–
0.25	F	Meningitis	–
0.75	F	SIDS	–
0.92	F	SIDS	–
6	F	Trauma	–
14	F	Pneumonia	–
19	F	Myelogenous leukemia	1.2
29	M	Cystic fibrosis	1.4
41	F	Hepatic failure	1.2
44	F	Respiratory failure	1.5
59	F	Legionella pneumonia	1.5
61	M	Amyotrophic lateral sclerosis	2.3
73	F	Parkinson's disease	0.9
76	M	Subdural hematoma	–

SIDS, sudden infant death syndrome

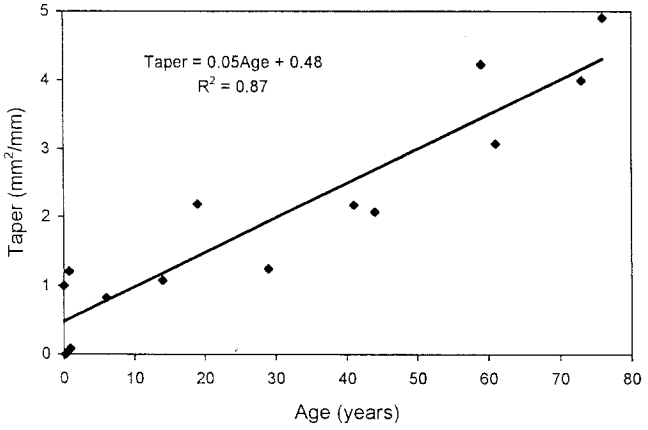

Fig. 1. Apical taper as a function of age. The area taper in the apical region increased linearly with increasing patient age ($P < 0.001$). No similar correlations were observed in either the pre- or postapical regions

Table 2. Change in area of the three regions

Age of patient (years)	Area change (%)		
	Preapical	Apical	Postapical
0.003	69.3	−19.2	6.4
0.25	29.8	−18.2	37.1
0.75	32.6	−45.6	31.5
0.92	17.8	−11.6	26.4
6	18.5	−8.7	8.8
14	22.2	−13.5	6.1
19	19.5	−6.0	16.9
29	13.9	−22.9	–
41	16.2	−28.9	3.7
44	18.5	−16.5	3.0
59	29.8	−9.9	4.7
61	11.1	−30.0	12.5
73	16.5	−37.7	3.1
76	28.8	−27.8	3.9
Mean ± SEM	24.6 ± 3.9	−21.2 ± 3.1	12.4 ± 3.4

The luminal boundary of the artery was outlined manually with approximately 50 points using a mouse. Luminal cross-sectional area was calculated based on the area enclosed between adjacent points on the boundary, while the location of the centroid was calculated by averaging all x- and all y-coordinates from the pixels that outlined the lumen.

Ellipticity was calculated from the ratio of the anteroposterior (AP) diameter to the lateral one. These were measured directly from the video-recorded images of the block face. As discussed later, this creates problems near the bifurcation where the lumen becomes biconcave.

Area taper was expressed as the change in area/unit length in units of mm^2/mm, and was defined as flare if the area increased distally and as taper if it decreased. In the circular or elliptical regions, it was also calculated as an angle using the relationship:

$$\tan(\theta) = \frac{(b_1 - b_2)}{\lambda},$$

where the diameter (b_n) was calculated from the luminal area (A) and the ellipticity factor of 0.9 (i.e., $b_n = \frac{A_n}{\sqrt{\pi(0.9)}}$, where n = 1 (proximal) or 2 (distal)). The angle could not be calculated with this formula where the shape was neither circular nor elliptical.

Wall thickness was measured radially in 15° increments from the centroid using a polar grid where 0° was right-lateral and 90° was anterior. The iliac arteries were cut obliquely and were corrected to the equivalent cross sections using the cosine of the half angle.

All data are presented as mean values ± standard error (SEM). Comparisons were made using t-tests and analysis of variance (ANOVA), and differences were significant if $P < 0.05$.

Results

The measured luminal area was overestimated by 4.0% ± 0.2% based on the analysis of test-patterns while wall thickness was underestimated by 3.1% ± 0.3%. These estimations were smaller than the biological variability and were ignored.

In most cases there were three regions: an apical region which correlated with the development of the branches just proximal to the bifurcation, a preapical region that extended from the renal arteries to the apical region, and a postapical region corresponding to the proximal part of the iliacs. The apical region tapered with an average are decrease of 21.2% ± 3.1%, while the other two regions flared with an area increase of 24.6% ± 3.9% in the preapical region and 13.3% ± 3.3% in the postapical region (Table 2). The latter two regions were significantly different ($P < 0.05$).

The lengths of each of the three regions (i.e., preapical, apical, postapical) were different. Consequently, the area changes were normalized to give taper (or flare) as an area/unit length. The flare was 3.58 (±0.87 mm^2/mm) in the preapical region, and 0.82 (±0.12 mm^2/mm) in the postapical region (Table 3). The preapical area flare corresponded to a flare angle of 1.96 (±0.43°). The apical region tapered with an area decrease/unit length of 2.96 (±0.80 mm^2/mm). Because of the shape changes in the apical and postapical regions, a taper angle could not be calculated.

The apical taper (in area/unit length) increased linearly with age. (Fig. 1). This age relationship was not observed with the flared regions pre- and postapically.

Ellipticity in the preapical region indicates that the AP diameter is always less than the lateral or transverse diameter (Fig. 2a,b). The lateral diameter has been reported previously by others using aortography. The degree of ellipticity increases as the bifurcation is approached, but the exact location of this change appears to be age-dependent (Fig. 2c). Ellipticity was assessed in the infrarenal aorta since the iliac branches were sectioned obliquely. In the apical region, the diameter ratio of the young subjects (i.e., those aged 1 day to 19 years) had quite a different shape than was found in subjects over 20 years of age because of the location of the change from circular to elliptical lumens.

Table 3. Area changes normalized as flares or tapers

Age of patient (years)	Preapical flare	Apical taper	Postapical flare
0.003	5.70	1.00	1.11
0.25	–	–	–
0.75	0.36	1.21	0.22
0.92	0.19	0.08	1.35
6	1.06	0.82	0.86
14	0.83	1.08	1.05
19	0.76	2.19	0.85
29	0.40	1.25	–
41	0.64	2.18	0.40
44	0.79	2.08	0.43
59	2.08	4.23	3.10
61	0.67	3.08	2.33
73	0.56	4.00	1.11
76	1.45	4.91	0.53
Mean ± SEM	3.58 ± 0.87	2.96 ± 0.80	0.82 ± 0.12

Flares and tapers reported have the units mm^2/mm.

The circumferential variations in preapical aortic wall thickness, plotted in polar coordinates, was measured in 11 of the 14 patients (Fig. 3a). Each data point represents the longitudinal-average wall thickness measured along the aorta normalized to the value obtained in the left-lateral region. Anterior and posterior wall thickness corresponded to 90° and 270°, respectively. The average wall thickness, and a circle of unit radius (i.e., $r = 1$ mm) have been superimposed on this plot for the sake of comparison. The circumferential-average wall thickness decreased between 0° (right lateral) and 120° while a significant increase in thickness was present between 120° and 200°. The most striking deviation was found in the 1-day-old patient (solid circle) which was very thin posteriorly. This might be due to the large flow in the umbilical circulation prior to delivery. If so, it is interesting how fast wall remodeling occurs as the posterior wall is not thinner in the other infants. The thickened

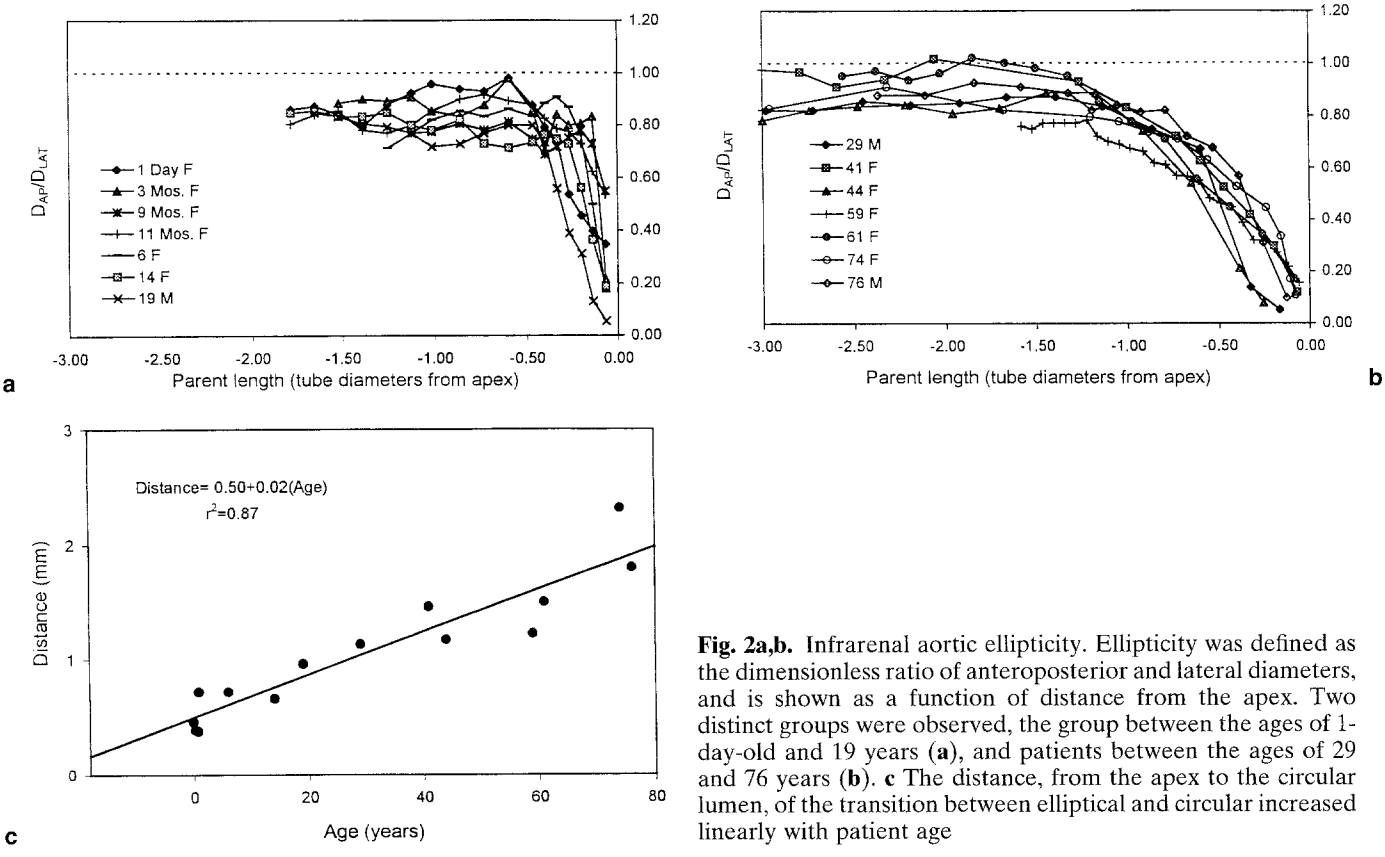

Fig. 2a,b. Infrarenal aortic ellipticity. Ellipticity was defined as the dimensionless ratio of anteroposterior and lateral diameters, and is shown as a function of distance from the apex. Two distinct groups were observed, the group between the ages of 1-day-old and 19 years (**a**), and patients between the ages of 29 and 76 years (**b**). **c** The distance, from the apex to the circular lumen, of the transition between elliptical and circular increased linearly with patient age

hypertensive aorta of the 61-year-old (upright triangle) appeared thickest in the right lateral region, but was considerably thinner than the average wall thickness on the left lateral side. None of these vessels had obvious atherosclerotic lesions.

Changes in wall thickness along the length of the parent branch from 4 of the 14 patients are shown in Fig 3b. Each data point represents the average thickness (±SEM) from 0° to 345°. In both the 0.003-year-old and the 0.75-year-old patients, there was no correlation be-

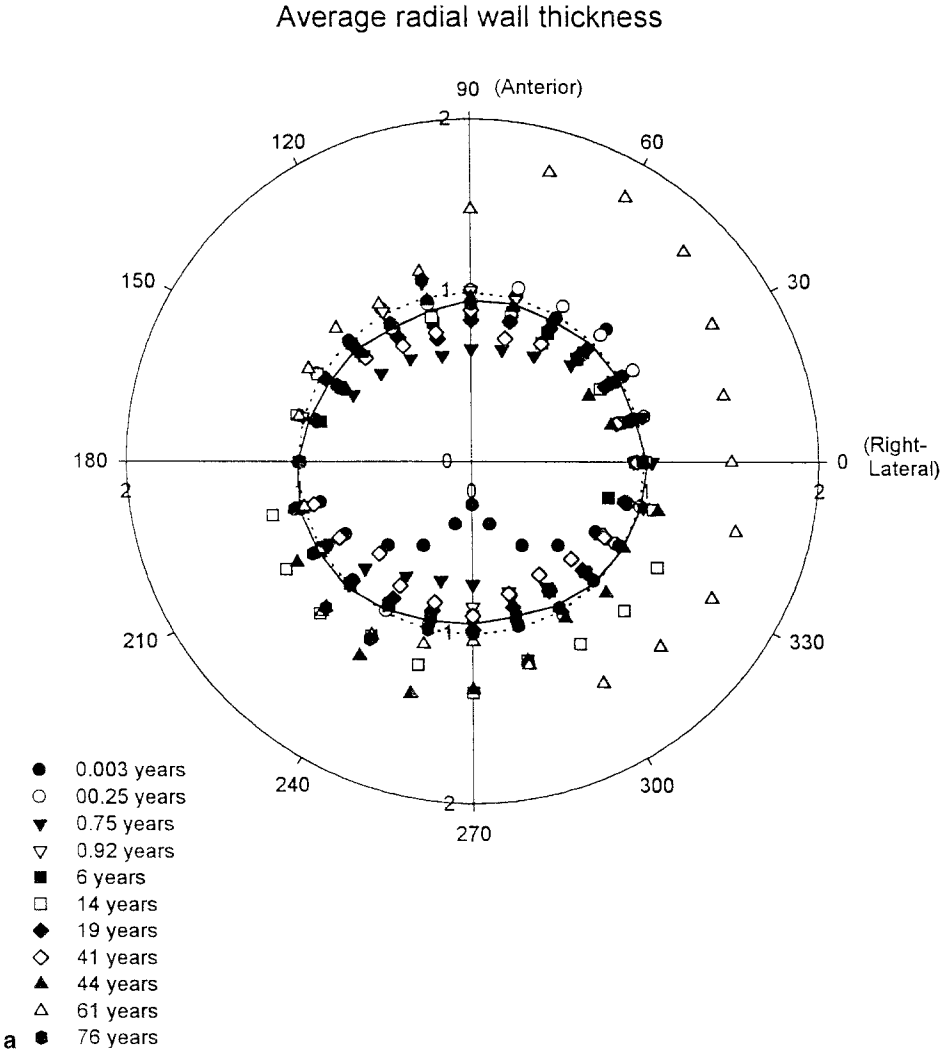

Fig. 3. a Average radial wall thickness is shown for 11 of the 14 patients using a polar coordinate map. In this plot, wall thickness was normalized to the value at the left-lateral position (180°). The average wall thickness of the 11 patients is shown with a *solid line* and is compared to a circle of unit radius (*dotted line*). **b** The longitudinal variation in radial wall thickness is shown for only 4 of the 14 patients for sake of clarity. Each data point represents the average (±SEM) variation in circumferential wall thickness (shown in a) as a function of distance from the apex

tween aortic length and wall thickness ($P > 0.05$). However, in each of the older patients, the parent branch was thickest furthest from the apex of the bifurcation and became thinner towards the apex.

Discussion

We have developed an accurate method to measure both luminal cross-sectional area and wall thickness at discrete locations along the human aortoiliac bifurcation. The 4% error attributed to video recording, digitizing, and measuring luminal area and wall thickness was considered to be negligible.

Several studies have used aortography to examine bifurcation geometry [5–7]. Aortography is advantageous compared with the sectioning technique that we have reported here since geometric measurements can be obtained in vivo, with proper tethering and under physiological conditions. As compared with the 14 patients that we have studied with serial sectioning, aortographic-based studies have examined hundreds of patients. Although aortography is probably valid for measuring branch angles, this technique only provides a two-dimensional cross-sectional view of the aorta, excluding the wall, through a region which is elliptical near the apex of the bifurcation.

This study has shown that both the infrarenal aorta and the proximal region of the iliacs flare significantly. This needs to be considered in future models that have assumed the aorta is circular in cross section and cylindrical along its length [9–11]. One would predict that this could lead to small regions of flow separation distally. Simplified theoretical fluid dynamic studies in our laboratory suggest that even small amounts of flare in straight tubes create flow separation and zones with decreased shear stress [12]. Detailed studies of changes in intimal thickness, and mapping of the precise location of atherosclerotic lesions taking flow separation into account, seem justified. Sundell and Roach [13] showed that the area of fatty lesions in unpressurized human aortas at autopsy were related to local differences in taper and flare.

If Zarins et al. [1] are correct that the lumen remodels to maintain a constant shear stress, this would imply that shear stress must vary along the length of the aorta, even in the absence of major branches. To our knowledge, this has not been considered in analyzing how lesion location is tied to shear stress.

Changes in lumen ellipticity in the apical region are probably tied to the need to produce a bifurcation rather than to flow factors. This idea is supported by the marked difference in the young (<20 years) and the old, in terms of where a constant ellipticity is reached (Fig. 3a). The same rationale may explain why the postapical region (i.e., the iliacs) flare away from the bifurcation as this flare seems related to the total angle of the branch. It is interesting that the maximum area in the human cerebral and porcine renal arteries we studied previously had their maximum area at the flow divider so that they flared along the parent and tapered along the branches.

Giddens et al. [13] have suggested that wall thickness was determined by tensile stress in the wall. Thus, if the wall tension was high (roughly equal to pressure x radius, according to Laplace's law), then the wall should become thicker as stress increases. The wall of the single hypertensive patient was thicker than all of the others studied, and supports this theory. Since Laplace's law assumes the wall is isotropic and cylindrical, it is hard to assess what one would predict would happen with ellipticity, particularly near branches.

In conclusion, this detailed geometric analysis suggests that taper, flare, and variations in both circumferential and longitudinal wall thickness need to be considered in trying to correlate physical forces in the aorta with the precise location of atherosclerotic lesions.

References

1. Zarins CK, Zatina MA, Giddens DP, Ku DN, Glagov S (1987) Shear stress regulation of artery lumen diameter in experimental atherogenesis. J Vasc Surg 5:413–420
2. Brownlee RD, Langille L (1991) Arterial adaptations to altered blood flow. Can J Physiol Pharmacol 69:978–983
3. MacLean NF, Kratky RG, Macfarlane TWR, Roach MR (1992) Taper: an important feature of Y-bifurcations in porcine renal arteries and human cerebral arteries. J Biomech 25:1047–1052
4. Macfarlane TWR (1985) A computer-based quantitative image analysis of geometry of human cerebral arterial bifurcations. PhD Thesis, University of Western Ontario, London, Ontario, pp 62–94
5. Seilly DJ (1982) A chemical test to determine the end point of EDTA decalcification. Med Lab Sci 39:71–73
6. Bargeron CB, Hutchins GM, Moore W, Deters OJ, Mark FF, Friedman MH (1986) Distribution of the geometrical parameters of human aortic bifurcations. Arteriosclerossis 6:109–113
7. Gosling RG, Newman DL, Bowden NLR, Twinn KW (1971) The area ratio of normal aortic junctions: aortic configuration and pulsewave reflection. Br J Radiol 44: 850–853
8. Lee Y-TN, Keitzer WF, Waston FR, Liu H (1982) Vascular geometry at the abdominal aortic bifurcation. JAMWA 37:77–81
9. Pedersen EM, Sung H-W, Burlson AC, Yoganathan AP (1993) Two-dimensional velocity measurements in a pulsatile flow model of the normal abdominal aorta simulating different hemodynamic coditions. J Biomech 26:1237–1247
10. Moore JE Jr, Maier SE, Ku DN, Boesiger P (1994) Hemodynamics in the abdominal aorta: a comparison of in vitro and in vivo measurements. J Appl Physiol 76:1520–1527

11. Peifer JW, Ku DN (1993) Computer modeling of the abdominal aorta using magnetic resonance images. Ann Biomed Eng 21:237–245
12. Mapara N (1996) A computer simulation of the effect of minor geometric perturbations on blood flow. MSc Thesis, The University of Western Ontario, London, Ontario, pp 24–42
13. Sundell PM, Roach MR (1998) The role of taper on the distribution of atherosclerosis in the human infra-renal aorta. Atherosclerosis (in press)
14. Giddens DP, Zarins CK, Glagov S (1993) The role of fluid mechanics in the localization and detection of atherosclerosis. J Biomech Eng 115:588–594